Available online at www.sciencedirect.com
ScienceDirect
Trans. Nonferrous Met. Soc. China 32(2022) 3434−3443
Transactions of Nonferrous Metals Society of China
www.tnmsc.cn

Effect of As(III) on kinetics of Fe^{2+} bio-oxidation

Qian WEI[1], Wen-qing QIN[1], Xue-duan LIU[1], Kai LIU[2], Cong-ren YANG[1]

1. School of Minerals Processing and Bioengineering, Central South University, Changsha 410083, China;
2. Scientific Research Academy of Guangxi Environmental Protection, Nanning 530022, China

Received 30 August 2021; accepted 31 March 2022

Abstract: Fe^{2+} bio-oxidation influenced by toxic metal ions released from the dissolution of arsenic-bearing gold ores was investigated. Fe^{2+} bio-oxidation by moderately thermophilic microorganisms was studied under different initial concentrations of Fe^{2+} and As(III), and Monod equation was used to fit the Fe^{2+} bio-oxidation under different conditions. Results showed that the Fe^{2+} bio-oxidation rate increased as the initial Fe^{2+} concentration increased until it reached 12 g/L. As(III) severely inhibited Fe^{2+} bio-oxidation. When the As(III) concentration was 8 g/L, 9 g/L Fe^{2+} was more than 200 h. The Monod equation fitted the Fe^{2+} bio-oxidation well. In the absence of As(III), the maximum specific growth rate of the culture and the substrate affinity constant were 0.142 h^{-1} and 0.053 g/L, respectively. As(III) inhibited Fe^{2+} bio-oxidation via competitive inhibition, and the inhibition constant was 0.0035 g/L.
Key words: moderately thermophilic microorganisms; Fe^{2+} bio-oxidation; As(III); As-bearing gold concentrate; kinetics

1 Introduction

Many gold-bearing deposits are sulphidic in nature and composed of invisible gold that is inaccessible to a cyanide solution [1]. They often contain gold particles that are finely disseminated in sulphide ores. Aside from pyrite, arsenopyrite is another common gold-bearing sulphide mineral. Compared with other pre-treatment technologies for refractory gold ores, biological oxidation is an effective method that enables concealed gold to be exposed for subsequent recovery and has certain advantages in terms of economy and environmental protection [2−4].

Fe^{2+} bio-oxidation is an important sub-process of the biological oxidation process and continuously provides Fe^{3+} as an oxidant for a catalytic cycle that increases the metal dissolution rate [5−7]. Bio-oxidation is a complex process that is related to physical, chemical and biological interactions, and it is affected by parameters such as pH, temperature, dissolved oxygen concentration and metal ion concentration. In industrial production, pH, temperature and dissolved oxygen concentration in a biologic oxidation tank can be maintained through online monitoring and regulation in the range of 1.0−1.5, 45−50 °C and around 5 mg/L, which are suitable for the growth of moderate thermophiles [8,9]. However, with the continuous dissolution of minerals, the concentrations of various metal ions, such as Fe^{2+}, Fe^{3+}, As(III) and As(V), in leaching solutions increase gradually, thereby affecting the growth and oxidation activity of microorganisms [10,11].

Given that arsenopyrite is the main mineral in most As-bearing gold concentrates, investigations on the effects of the initial concentrations of metal ions such as Fe^{2+}, Fe^{3+} and As(III) on microbial growth and Fe^{2+} bio-oxidation help to predict the Fe^{2+} bio-oxidation rate under different initial conditions and compare the inhibition degrees of

Corresponding author: Cong-ren YANG, Tel: +86-731-88830884, E-mail: yangcongren@csu.edu.cn;
Kai LIU, Tel: +86-731-88830884, E-mail: 121512346@qq.com
DOI: 10.1016/S1003-6326(22)66030-8

the metal ions on Fe^{2+} bio-oxidation [12,13]. The effects of heavy metal ions on microbial growth and Fe^{2+} bio-oxidation have been fully elucidated and discussed [14,15]. Many Fe^{2+} oxidation kinetic studies have mostly been conducted with mesophilic microorganisms [16,17], and the inhibition kinetic model of Fe^{3+} on Fe^{2+} bio-oxidation has been proposed [18,19]. However, few Fe^{2+} bio-oxidation kinetic studies have been performed with a mixed moderately thermophilic culture [9,17,20], and the inhibition type of As(III) on Fe^{2+} bio-oxidation has not been determined [21,22].

Therefore, this work was conducted to investigate the effect of As(III) on the kinetics of Fe^{2+} bio-oxidation by a mixed moderately thermophilic culture. The effect of different initial concentrations of Fe^{2+} and As(III) on Fe^{2+} bio-oxidation was studied, and the kinetic models of Fe^{2+} bio-oxidation in the presence of Fe^{2+} and As(III) were developed. The inhibition degrees of different metal ions on Fe^{2+} bio-oxidation were compared, and the Fe^{2+} bio-oxidation rate under different initial conditions was predicted.

2 Experimental

2.1 Microorganisms and culture media

The mixed moderately thermophilic micro-organisms used in this study were collected from the leaching solution of a sulphide copper heap leaching operation in the Inner Mongolia Autonomous Region, China. After adaptation to a high As-bearing gold concentrate for 2 years, this culture could tolerate more than 7 g/L As(III). Two distinct clones were sequenced through 16S rDNA gene amplification the establishment of a clone library, amplified ribosomal DNA restriction analysis and amplified 16S rDNA sequencing. The results indicated that one clone shared 99% identity with *Sulfobacillus thermosulfidooxidans* DSM 9293 (a ferrous iron and sulfur oxidiser) [23], and the second clone shared 96% identity with *Acidithiobacillus caldus* DSM 8584 (a sulphur oxidiser but not a ferrous iron oxidiser) [24]. The culture was enriched and grown in 100 mL of 9K basal salt medium at pH 1.2 in 250 mL shake flasks by using a rotary shaker (rotational speed: 300 r/min) at 45 °C. The 9K basal salt medium was composed of the following compounds: 3 g/L $(NH_4)_2SO_4$, 0.5 g/L K_2HPO_4, 0.5 g/L $MgSO_4 \cdot 7H_2O$, 0.1 g/L KCl and 0.01 g/L $Ca(NO_3)_2$ [25]. The moderately thermophilic microorganisms were supplemented with 0.01% yeast extract. The microbial culture was sub-cultured into basal salt medium supplemented with 2% As-bearing concentrate as an energy source. The suspension containing microbial cells was harvested and centrifuged at 9000 r/min for 20 min, and the collected cells were suspended in 9K basal salt medium without any energy source for the experiments.

2.2 Methods

2.2.1 Fe^{2+} bio-oxidation experiments

Fe^{2+} bio-oxidation experiments were performed in a 1.5 L mechanically stirred reactor with a stirrer speed of 300 r/min at 48 °C. Then, 1.0 L of 9K basal salt medium was added to the reactor, and the air injection rate was adjusted to 1 L/min. The microorganism culture was inoculated to obtain an initial cell concentration of 10% (volume fraction). The initial pH was adjusted to 1.2 with 20% H_2SO_4. The culture was exposed to different Fe^{2+} and As(III) concentrations to study the effects of Fe^{2+} and As(III) on the microbial growth and Fe^{2+} bio-oxidation. Solution samples were periodically withdrawn and measured to determine the Fe^{2+} and cell concentrations. Sampling loss was compensated by adding the same volume of iron-free 9K basal salt medium, and the evaporation loss was supplemented with distilled water (pH 1.2).

2.2.2 Analytical methods

The solution pH values were measured with a PHSJ−4A type pH meter by using a pH composite electrode (65-1 type). The Fe^{2+} and As(III) concentrations were measured by titration with cerium sulphate [22]. In cerium sulphate titration, under a certain concentration of mixed sulphur acid–phosphorus system, sodium diphenylamine sulphonate was used as an indicator, and ferrous iron was titrated with a standard solution of cerium sulphate. The cell concentration in the leaching solution was measured by using a haemocytometer (Shanghai Qiujing Biochemical Reagent Instrument Co., Ltd) and a binocular electron microscope (Olympus CX31, Shanghai Fenye Optoelectronic Equipment Co., Ltd).

2.2.3 Establishment of kinetic model of Fe^{2+} bio-oxidation

In a microbial batch culture system, microbial cell autolysis can usually be disregarded because of its short cycle. Therefore, the growth of cells can be expressed as [17,26]

$$\frac{\mathrm{d}X}{\mathrm{d}t}=\mu X \tag{1}$$

where X is the cell concentration (cell/L); t is the growth time (h); and μ is the cell specific growth rate (h^{-1}).

μ is proportional to X and not a constant in a batch culture system. It is related to restrictive medium conditions, such as temperature, dissolved oxygen concentration, pH and substrate concentration. In this study, the dissolved oxygen concentration, temperature and pH of the medium could be kept constant. Therefore, μ is related to the substrate concentration, that is, to the Fe^{2+} concentration. The Monod equation is the most frequently used expression for microbial growth [18,27,28], as

$$\mu=\frac{\mu_{\max}S}{K_{\mathrm{s}}+S} \tag{2}$$

where $\mu_{\max}$ is the maximum specific growth rate (h^{-1}); S is the Fe^{2+} concentration (g/L); K_{s} is the substrate affinity constant (g/L); $\mu_{\max}$ and K_{s} vary with the culture temperature and ionic strength of the medium [27,29].

As(III) inhibits microbial growth when As(III) is added to the medium. Under this condition, the Monod equation cannot describe the cell growth well, and a term reflecting the influence of the inhibitor must be added. The inhibition type of As(III) on Fe^{2+} bio-oxidation has not been determined, so the Monod equation should be rewritten into a competitive inhibition type, as shown in Eq. (3), after the addition of As(III) to the medium, or it should be rewritten into a noncompetitive inhibition type, as presented in Eq. (4). The inhibition type must be determined by comparing how well the two models fit the experimental data:

$$\mu=\frac{\mu_{\max}S}{K_{\mathrm{s}}(1+[\mathrm{As}^{3+}]/K_{\mathrm{i}})+S} \tag{3}$$

$$\mu=\frac{\mu_{\max}S}{(K_{\mathrm{s}}+S)(1+[\mathrm{As}^{3+}]/K_{\mathrm{ii}})} \tag{4}$$

where $[As^{3+}]$ is the As(III) concentration (g/L); K_{i} is the competitive inhibition constant (g/L); K_{ii} is the noncompetitive inhibition constant (g/L).

Yield coefficient (Y), which was proposed by PANIKOV [30], is used to describe the relationship between substrate consumption and microbial cell growth, that is, the mass of microbial cells produced by consuming a unit mass of substrate, is expressed as

$$\frac{\mathrm{d}S}{\mathrm{d}t}=-\frac{1}{Y}\cdot\frac{\mathrm{d}X}{\mathrm{d}t} \tag{5}$$

Equation (6) is obtained by integrating Eq. (5):

$$Y=\frac{X-X_0}{S_0-S} \tag{6}$$

where X_0 is the initial cell concentration, and S_0 is the initial Fe^{2+} concentration.

Equations (7) is obtained from Eqs. (1), (5) and (6):

$$\frac{\mathrm{d}S}{\mathrm{d}t}=-\frac{\mu}{Y}\cdot[X_0+Y(S_0-S)] \tag{7}$$

Equations (8)−(10) are obtained by substituting Eqs. (2)−(4) into Eq. (7), respectively,

$$\frac{\mathrm{d}S}{\mathrm{d}t}=-\frac{\mu_{\max}S[X_0+Y(S_0-S)]}{Y(K_{\mathrm{s}}+S)}$$

(in the absence of an inhibitor) (8)

$$\frac{\mathrm{d}S}{\mathrm{d}t}=-\frac{\mu_{\max}S[X_0+Y(S_0-S)]}{Y[K_{\mathrm{s}}(1+[\mathrm{As}^{3+}]/K_{\mathrm{i}})+S]}$$

(competitive inhibition by As(III)) (9)

$$\frac{\mathrm{d}S}{\mathrm{d}t}=-\frac{\mu_{\max}S[X_0+Y(S_0-S)]}{Y(K_{\mathrm{s}}+S)(1+[\mathrm{As}^{3+}]/K_{\mathrm{ii}})}$$

(noncompetitive inhibition by As(III)) (10)

Within the range of t_0−t and S_0−S, the relationship formula of the Fe^{2+} concentration with time is obtained using the mathematical software Maxima to integrate Eqs. (8)−(10), as shown in Eqs. (11)−(13), respectively. Equations (11)−(13) establish the relationship between the Fe^{2+} concentration and the kinetic parameters ($\mu_{\max}$, Y, K_{s}, K_{i}, K_{ii}) of microbial growth. According to Eq. (6), the yield coefficient (Y) can be plotted on X_0−X and S_0−S under various initial concentrations of Fe^{2+} and As(III). The slope of the straight line obtained by linear fitting is Y. According to the change of the Fe^{2+} concentration as a function of

time, the parameters (μ_{max}, K_s, K_i, K_{ii}) can be calculated using the nonlinear fitting software package of MATLAB 7.0.

$$\mu_{max}t=\frac{(S_0+K_s)Y+X_0}{S_0Y+X_0}\cdot\ln\frac{S_0Y-SY+X_0}{X_0}+\frac{YK_s}{S_0Y+X_0}\cdot\ln\frac{S_0}{S}$$

(in the absence of inhibitor) (11)

$$\mu_{max}t=[\frac{(S+K_s+[As^{3+}]K_s/K_i)Y+X_0}{S_0Y+X_0}\cdot\ln\frac{S_0Y-SY+X_0}{X_0}]+[\frac{([As^{3+}]+K_s)Y}{S_0Y+X_0}\ln\frac{S_0}{S}]$$

(competitive inhibition by As(III)) (12)

$$\mu_{max}t=(1+\frac{[As^{3+}]}{K_{ii}})[\frac{(S_0+K_s)Y+X_0}{S_0Y+X_0}\cdot\ln\frac{S_0Y-SY+X_0}{X_0}+\frac{YK_s}{S_0Y+X_0}\cdot\ln\frac{S_0}{S}]$$

(noncompetitive inhibition by As(III)) (13)

3 Results and discussion

3.1 Fe^{2+} bio-oxidation by mixed moderately thermophilic culture

3.1.1 Effect of initial Fe^{2+} concentration on Fe^{2+} bio-oxidation

Figure 1 shows Fe^{2+} bio-oxidation (a) and microbial cell growth (b) as a function of various initial Fe^{2+} concentrations. As shown in Fig. 1, the lag phase of the microorganisms gradually increased as the initial Fe^{2+} concentration increased from 1 to 10 g/L. When the Fe^{2+} concentration was less than 5 g/L, the lag phase was not obvious, and Fe^{2+} could be completely oxidized within 18 h. When the Fe^{2+} concentration increased to 10 g/L, the lag phase reached 10 h, and Fe^{2+} was completely oxidized in 22 h. After the exponential phase, the oxidation rate (the slope of the Fe^{2+} oxidation curve) increased as the initial Fe^{2+} concentration increased. When the initial Fe^{2+} concentration reached 10−12 g/L, the Fe^{2+} oxidation rate did not change remarkably. The results indicated that the increase in the Fe^{2+} concentration did not inhibit Fe^{2+} oxidation by the microorganisms within the initial Fe^{2+} concentration (1−12 g/L).

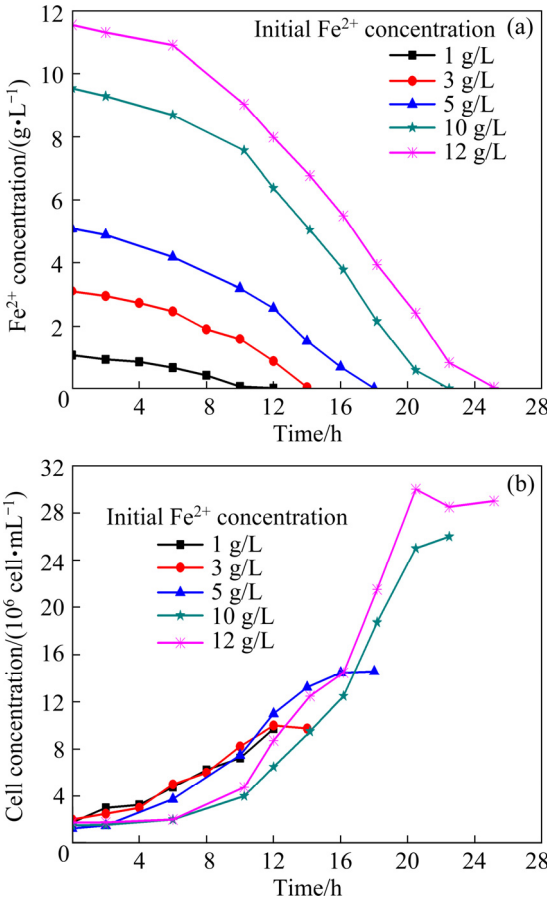

Fig. 1 Fe^{2+} bio-oxidation (a) and microbial cell growth (b) under various initial Fe^{2+} concentrations with pH 1.2 at 48 °C

3.1.2 Effect of As(III) concentration on Fe^{2+} bio-oxidation

According to previous studies [31,32], in the biological pre-oxidation of As-bearing gold ores, As(III) is released into an aqueous solution, thus harming microbial cell growth and inhibiting the oxidation activity of the microorganisms. Figure 2 shows Fe^{2+} bio-oxidation (a) and microbial cell growth (b) under various As(III) concentrations. The results revealed that the Fe^{2+} oxidation rate greatly declined as As(III) was added (Fig. 2(a)) compared with that in the case without As(III) (Fig. 1(a)). The time required for complete Fe^{2+} oxidation increased from 45 h in the presence of 1 g/L As(III) to 200 h in the presence of 8 g/L As(III). As shown in Fig. 2(b), the addition of As(III) affected the microbial cell growth. The higher the As(III) concentration, the lower the cell concentration. As(III) inhibited microbial growth because As(III) bound to active sulphydryl groups of most enzymes (including enzymes in the

respiratory chain) to inactivate enzymes, thereby obstructing cell metabolism [1,33]. The results also demonstrated that the microorganisms could still oxidize Fe^{2+} in the presence of 8 g/L As(III). However, low As(III) concentrations must be maintained to improve the oxidation efficiency of Fe^{2+}.

3.2 Kinetics of Fe^{2+} bio-oxidation

3.2.1 Effects of different metal ions on microbial cell yield

Microbial cell yield is an important parameter of Fe^{2+} bio-oxidation kinetics, and it refers to microbial cell growth after a unit mass of Fe^{2+} is consumed [17]. The change in cell concentrations (X_0−X) versus that in Fe^{2+} concentrations (S_0−S) was plotted according to Eq. (6), as shown in Fig. 3, to obtain the yield coefficient (Y) of microorganisms under different initial concentrations of Fe^{2+} and As(III). The points (experimental results) in Figs. 3(a) and (b) were calculated by the experimental results in Figs. 1 and 2, respectively. The initial Fe^{2+} concentration increased from 1 to 12 g/L (Fig. 3(a)), whereas the concentration was 10 g/L (Fig. 3(b)). The slope (Y) of the fitting line was the yield coefficient of Fe^{2+} bio-oxidation (Tables 1 and 2). From Tables 1 and 2, Y with the addition of As(III) was lower than that without As(III). As the As(III) concentration in the growth environment increased, the energy obtained by Fe^{2+} oxidation could not be fully used for cell growth and reproduction, leading to decreased microbial cell yield. When the As(III) concentration increased from 1 to 3 g/L, the time required for complete 10 g/L Fe^{2+} oxidation increased from 44 h with the initial 1 g/L As(III) to 82 h with the initial 3 g/L As(III). The change in the cell concentration (X_0−X) decreased from 20.02 (10^9 cell/L) to 18.36 (10^9 cell/L). Therefore, Y obviously decreased from 2.135×10^9 cell/g to 1.82×10^9 cell/g. As the As(III) concentration continued to increase from 3 to 8 g/L, the increase in the cell concentration was

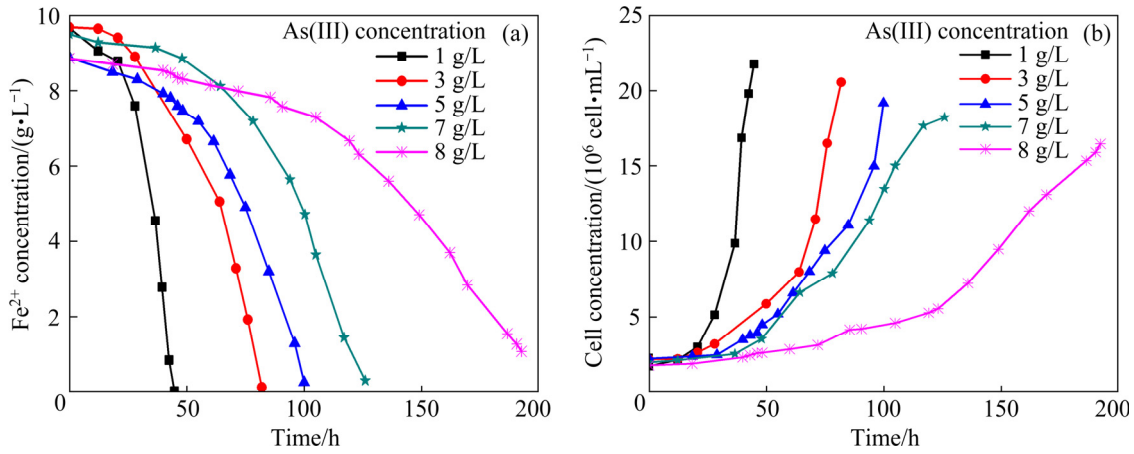

Fig. 2 Fe^{2+} bio-oxidation (a) and microbial cell growth (b) under various As(III) concentrations at pH 1.2 and 48 °C

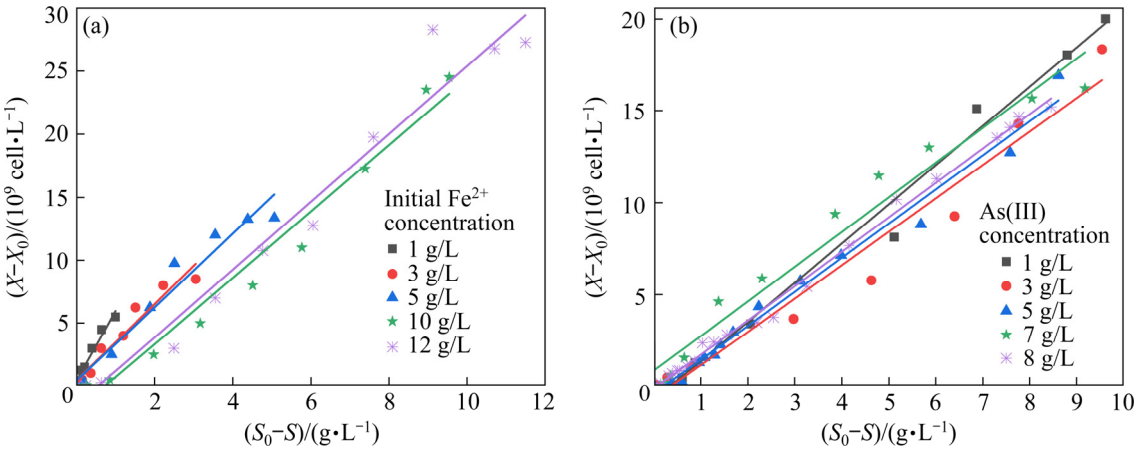

Fig. 3 Determination of yield coefficient (Y) by linear fitting of data under various initial concentrations of Fe^{2+} (a) and As(III) (b) with pH 1.2 at 48 °C (Point−Experimental; Line−Fitting results)

Table 1 Microbial yield coefficient (Y) under various initial Fe^{2+} concentrations

Initial Fe^{2+} concentration/(g·L^{-1})	Y/(10^9 cell·g^{-1})	R^2
1	5.55	0.95
3	3.04	0.93
5	2.92	0.95
10	2.63	0.97
12	2.68	0.96

Table 2 Microbial yield coefficient (Y) under various initial As(III) concentrations

As(III) concentration/(g·L^{-1})	Y/(10^9 cell·g^{-1})	R^2
1	2.13	0.98
3	1.82	0.96
5	1.86	0.98
7	1.89	0.96
8	1.87	0.99

gradually reduced, and the time required for complete Fe^{2+} oxidation increased to 200 h in the presence of 8 g/L As(III). According to the fitting results in Tables 1 and 2, Y slightly changed and was maintained in the range of (1.8−1.9)×10^9 cell/g.

3.2.2 Kinetic parameters of Fe^{2+} bio-oxidation under various initial Fe^{2+} concentrations

According to Fe^{2+} bio-oxidation data under various initial Fe^{2+} concentrations and the corresponding yield coefficients (Y) in Table 1, the kinetic parameters (μ_{max}=0.142 h^{-1} and K_s= 0.053 g/L) of microbial growth were obtained by using Eq. (11) to perform nonlinear fitting of the Fe^{2+} oxidation curves at different initial Fe^{2+} concentrations. After compiling the kinetic parameters (μ_{max} and K_s) available in the literature for the growth of *Acidithiobacillus ferooxidans*, NEMATI et al [20] pointed out discrepancies in the reported kinetic parameters. LIU et al [34] reported μ_{max}=0.11 h^{-1} for *Thiobacillus ferooxidans* with pH 1.8 at 35 °C. GOMES and CANTERO [35] observed μ_{max} as 0.14 h^{-1}. BOGDANOVA et al [36] observed a higher value of μ_{max} (0.35 h^{-1}) for *Sulfobacillus* in the presence of 9.82 g/L $FeSO_4·7H_2O$ at the optimum temperature of 40 °C. The value of μ_{max} in this work was lower than that (0.25 h^{-1}) achieved by PINA et al [17] in the Fe^{2+} concentration range of 10−20 g/L. Furthermore, K_s in this work was much lower (0.053 g/L versus 0.396 g/L). VITAYA et al [37] also demonstrated that the growth of *Sulfolobus acidocaldarius* has lower values of μ_{max}= 0.06 h^{-1} and K_s= 0.04 g/L.

The kinetic parameters (μ_{max} and K_s), initial Fe^{2+} concentrations (S_0), initial cell concentrations (X_0) and yield coefficients (Y) were substituted into Eq. (13) under various initial Fe^{2+} concentrations to test the accuracy of the obtained model parameters. Then, the theoretical curve of the change in Fe^{2+} concentrations under various initial Fe^{2+} concentrations was plotted with Origin 8.0 (Fig. 4). The determination coefficients (R^2) corresponding to different Fe^{2+} concentrations (1−12 g/L) were 0.93, 0.71, 0.94, 0.99 and 0.92, respectively (Fig. 4). Therefore, the calculated values of the model was in good agreement with the experimental values.

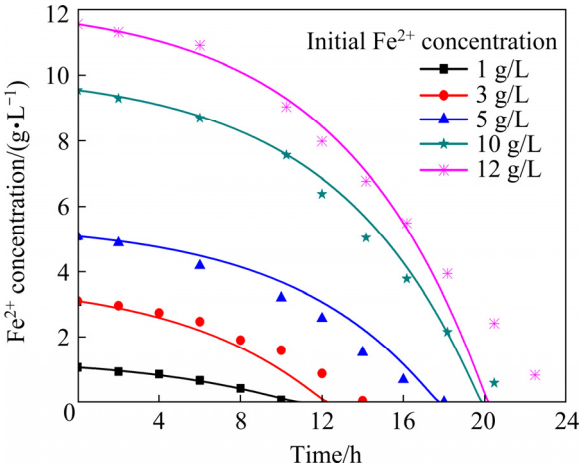

Fig. 4 Fitting of Fe^{2+} bio-oxidation under various Fe^{2+} concentrations with pH 1.2 at 48 °C

The change in the Fe^{2+} concentration as a function of the incubation time under different initial conditions could be predicted theoretically based on the kinetic parameters of microbial growth. For example, when the initial Fe^{2+} concentration was 10 g/L, and μ_{max} and K_s were substituted into Eq. (11), the relationship between Fe^{2+} concentrations and incubation time could be expressed as

$$0.142t = \frac{2.63(10+0.053)+X_0}{10\times 2.63+X_0}\cdot \ln\frac{10\times 2.63-2.63S+X_0}{X_0}+\frac{2.63\times 0.053}{10\times 2.63+X_0}\ln\frac{10}{S} \quad (14)$$

The calculated Fe^{2+} concentration with various initial cell concentrations (inoculation amount) is

shown in Fig. 5. The Fe^{2+} concentration increased as the initial cell concentration increased, that is, the larger the inoculation amount, the faster the Fe^{2+} bio-oxidation rate.

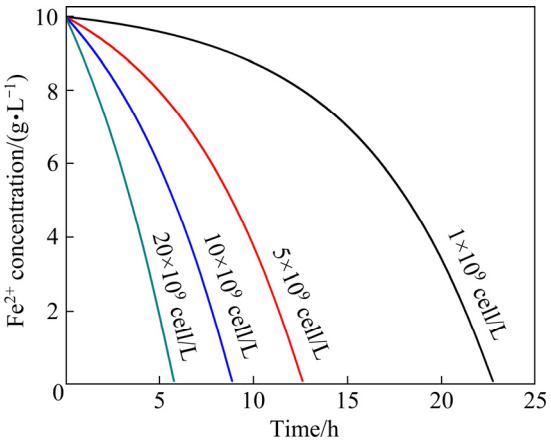

Fig. 5 Theoretical prediction of Fe^{2+} bio-oxidation under various initial cell concentrations (S_0=10 g/L, μ_{max}=0.142 h^{-1}, K_s= 0.053 g/L, Y=2.63×10^9 cell/g)

Fe^{2+} concentration with the time was plotted by changing different kinetic parameters (μ_{max} and K_s) in the kinetic model of microbial growth. This approach could predict the effect of changes in μ_{max} and K_s on the Fe^{2+} bio-oxidation rate (Figs. 6 and 7, respectively). The Fe^{2+} oxidation rate increased as μ_{max} increased, indicating that the faster the bacteria grew, the faster the Fe^{2+} became oxidized (Fig. 6). The substrate affinity constant (K_s) represented the affinity between enzymes and substrates. The smaller the value of K_s, the stronger the affinity between the enzymes and substrates. According to Fig. 7, Fe^{2+} oxidation rate declined as K_s increased,

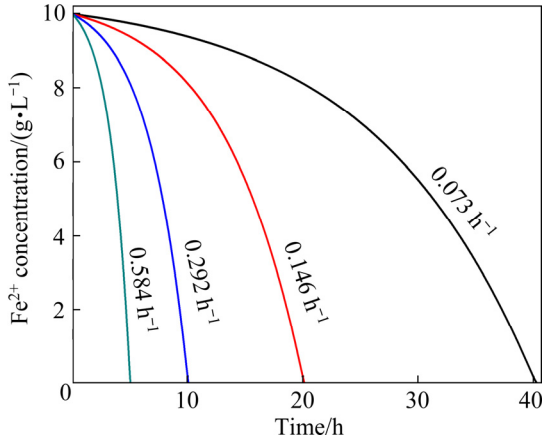

Fig. 6 Theoretical prediction of effect of μ_{max} on Fe^{2+} bio-oxidation (S_0=10 g/L, X_0=1.5×10^9 cell/L, K_s= 0.053 g/L, Y= 2.63×10^9 cell/g)

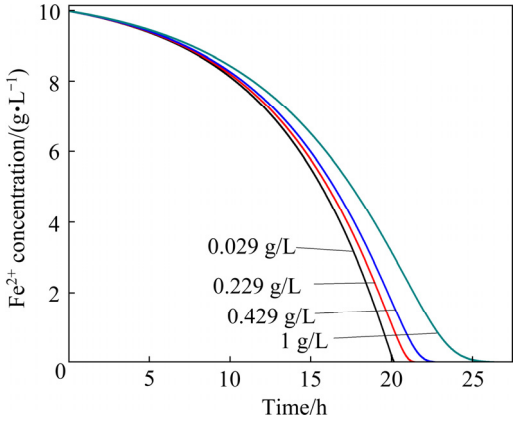

Fig. 7 Theoretical prediction of effect of K_s value change on Fe^{2+} bio-oxidation (S_0=10 g/L, X_0=1.5×10^9 cell/L, μ_{max}=0.142 h^{-1}, Y=2.63×10^9 cell/g)

indicating that the affinity between Fe^{2+} and Fe^{2+} oxidase decreased, and vice versa. The results showed that the combination of Fe^{2+} and Fe^{2+} oxidase was affected in the presence of toxic substances in the medium, resulting in decreased Fe^{2+} concentration.

3.2.3 Kinetic parameters of Fe^{2+} bio-oxidation under various As(III) concentrations

Few studies [18,19] have explored the effect of As(III) on the kinetics of Fe^{2+} bio-oxidation, but they have not determined the inhibition type of As(III) in Fe^{2+} oxidation. A competitive inhibition model (Eq. (12)) and a noncompetitive inhibition model (Eq. (13)) were used to fit the experimental data of Fe^{2+} bio-oxidation. The type of As(III) inhibition could be determined by comparing how well the two models fit the experimental data.

In the medium supplemented with As(III), the lag phase of the microorganisms was relatively long (Fig. 2). During the lag phase, Fe^{2+} bio-oxidation and microbial growth were not obvious and did not conform to the microbial growth kinetic model. Therefore, only the data in the exponential phase of microbial growth could be fitted to obtain the kinetic parameters of microbial growth.

According to the Fe^{2+} bio-oxidation data under various As(III) concentrations in the exponential phase in Fig. 2 and the corresponding yield coefficients (Y) in Table 1, Eqs. (12) and (13) were used to perform nonlinear fitting of the Fe^{2+} oxidation curves under various As(III) concentrations, respectively. The kinetic parameters of microbial growth obtained by nonlinear fitting of the competitive inhibition model (Eq. (12)) were as

follows: μ_{max}=0.142 h^{-1}, K_s=0.053 g/L, and K_i= 0.0035 g/L. The determination coefficients (R^2) of 1, 3, 5, 7 and 8 g/L As(III) were 0.994, 0.996, 0.822, 0.975 and 0.991, respectively. By comparison, the kinetic parameters obtained by nonlinear fitting of the noncompetitive inhibition model (Eq. (13)) were as follows: μ_{max}=0.142 h^{-1}, K_s=0.053 g/L, and K_{ii}=0.71 g/L. Likewise, for 1, 3, 5, 7 and 8 g/L As(III), R^2 is 0.794, 0.915, 0.981, 0.928 and 0.973, respectively. The fitting results of the competitive inhibition model were better than those of the noncompetitive inhibition model. Therefore, As(III) inhibited Fe^{2+} oxidation via competitive inhibition in the As(III) concentration range of 1−8 g/L (Fig. 8).

The relationship between the As(III) concentrations and the Fe^{2+} oxidation rate could be obtained on the basis of the competitive inhibition model (Eq. (9)), Y and the kinetic parameters (μ_{max}, K_s and K_i) of microbial growth obtained by nonlinear fitting. The theoretical Fe^{2+} oxidation rate as a function of As(III) concentration at the initial Fe^{2+} concentration of 10 g/L and the initial cell concentration of 1×10^7 cell/mL is presented in Fig. 9. After Eqs. (8) and (9) were compared, when As(III) was added, K_s in Eq. (8) was replaced by $K_s(1+[As^{3+}]/K_i)$, which was equivalent to the increase in the substrate affinity constant. This finding indicated that the affinity of Fe^{2+} and Fe^{2+} oxidase was reduced, resulting in a decreased Fe^{2+} oxidation rate. The theoretical Fe^{2+} oxidation rate was 0.265 g/(L·h) at the As(III) concentration of 1 g/L (Fig. 9) and decreased remarkably to 0.089 g/(L·h) (5 g/L As(III)). Then, it gradually declined to 0.0579 g/(L·h) (8 g/L As(III)); obviously, the decrement gradually declined.

The kinetic evaluation of Fe^{2+} bio-oxidation in the presence of different metal ions is one of the keys to reactor design because the kinetics must be considered in the determination of residence time and dimension. The results showed that the kinetic models were applicable to Fe^{2+} bio-oxidation as long as the kinetic parameters were determined for special metal ions and the microorganisms. Moreover, the inhibition degree of different metal ions on Fe^{2+} bio-oxidation may be compared and Fe^{2+} bio-oxidation may be theoretically predicted under different initial conditions. Consequently, a reference could be provided for the scale-up of bio-oxidation reactors and the control of process conditions. However, for different raw materials and leaching systems, the adaptability and tolerance of microorganisms differ. Therefore, in future investigations, the effects of different metal ions on Fe^{2+} bio-oxidation process by microorganisms should be explored in combination with production practice.

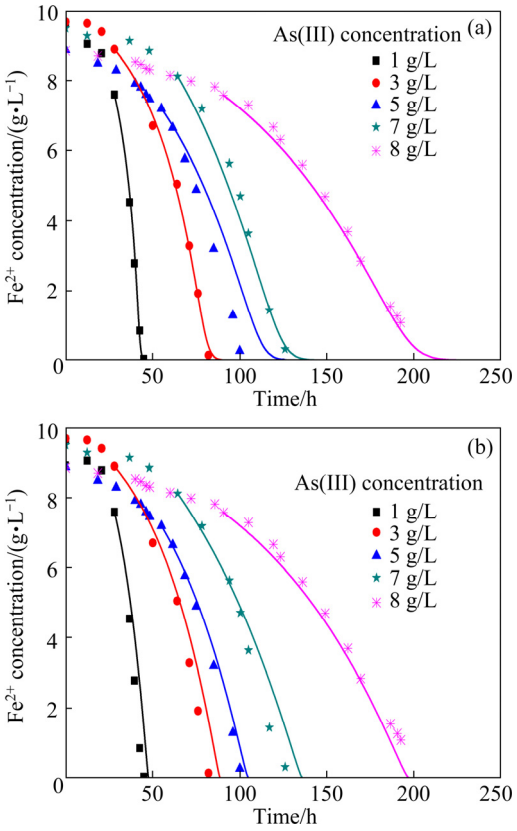

Fig. 8 Fitting of Fe^{2+} bio-oxidation with competitive inhibition model (a) and noncompetitive inhibition model (b) under various As(III) concentrations with pH 1.2 at 48 °C

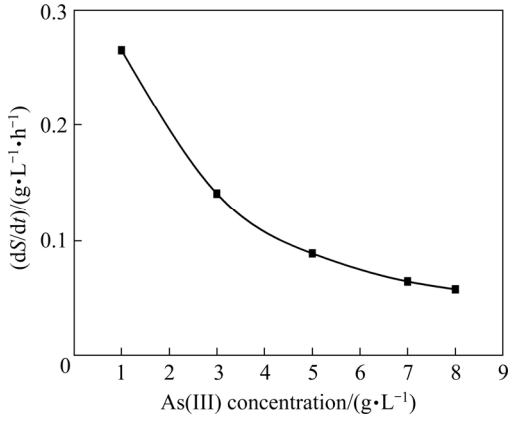

Fig. 9 Fe^{2+} oxidation rate at various As(III) concentrations (initial Fe^{2+} concentration: 10 g/L; initial cell concentration: 1×10^7 cell/mL)

4 Conclusions

(1) The Fe^{2+} bio-oxidation rate increased as the initial Fe^{2+} concentration in the medium increased until the Fe^{2+} concentration reached 12 g/L. The Fe^{2+} bio-oxidation rate was severely inhibited by As(III). When the As(III) concentration was 8 g/L, Fe^{2+} oxidation was completely oxidized more than 200 h.

(2) Microbial growth and Fe^{2+} bio-oxidation conformed to the Monod equation. According to the kinetic model of Fe^{2+} bio-oxidation, the kinetic parameters of Fe^{2+} bio-oxidation were obtained through nonlinear fitting. Under different initial Fe^{2+} concentrations, the maximum specific growth rate constant (μ_{max}) was 0.142 h^{-1}, and the substrate affinity constant (K_s) was 0.053 g/L. As(III) inhibited Fe^{2+} bio-oxidation through competitive inhibition. Under different As(III) concentrations, μ_{max} was 0.142 h^{-1}, K_s was 0.053 g/L, and the competitive inhibition constant (K_i) was 0.0035 g/L.

(3) This study could predict and compare the inhibition degree of different metal ions on Fe^{2+} biological oxidation. It also provides a reference for further studies and scale-up of biological oxidation reactors.

Acknowledgments

This work was supported by the National Natural Science Foundation of China (No. 51904339), and the Collaborative Innovation Center for Clean and Efficient Utilization of Strategic Metal Mineral Resources, China.

References

[1] CORKHILL C L, VAUGHAN D J. Arsenopyrite oxidation—A review [J]. Applied Geochemistry, 2009, 24: 2342−2361.

[2] de CARVALHO L C, DA SILVA S R, GIARDINI R M N, de SOUZA L F C, LEÃO V A. Bio-oxidation of refractory gold ores containing stibnite and gudmundite [J]. Environmental Technology & Innovation, 2019, 15: 100390.

[3] GAN M, JIE S Q, LI M M, ZHU J Y, LIU X X. Bioleaching of multiple metals from contaminated sediment by moderate thermophiles [J]. Marine Pollution Bulletin, 2015, 97: 47−55.

[4] XIE F, CHEN Jun-nan, WANG Jian, WANG Wei. Review of gold leaching in thiosulfate-based solutions [J]. Transactions of Nonferrous Metals Society of China, 2021, 31(11): 3506−3529.

[5] NYEMBWE K J, FOSSO-KANKEU E, WAANDERS F, MKANDAWIRE M. pH-dependent leaching mechanism of carbonatitic chalcopyrite in ferric sulfate solution [J]. Transactions of Nonferrous Metals Society of China, 2021, 31: 2139−2152.

[6] ZHAO C X, YANG B J, WANG X X, ZHAO H B, GAN M, QIU G Z, WANG J. Catalytic effect of visible light and Ca^{2+} on chalcopyrite bioleaching [J]. Transactions of Nonferrous Metals Society of China, 2020, 30(4): 1078−1090.

[7] COUDERT L, BONDU R, RAKOTONIMARO T V, ROSA E, GUITTONNY M, NECULITA C M. Treatment of As-rich mine effluents and produced residues stability: Current knowledge and research priorities for gold mining [J]. Journal of Hazardous Materials, 2020, 386: 121920.

[8] WANG J, TAO L, ZHAO H B, HU M H, ZHENG X H, PENG H, GAN X W, XIAO W, CAO P, QIN W Q, QIU G Z, WANG D Z. Cooperative effect of chalcopyrite and bornite interactions during bioleaching by mixed moderately thermophilic culture [J]. Minerals Engineering, 2016, 95: 116−123.

[9] NEMATI M, HARRISON S T L. A comparative study on thermophilic and mesophilic biooxidation of ferrous iron [J]. Minerals Engineering, 2000, 13: 19−24.

[10] VELOSO T C, SICUPIRA L C, RODRIGUES L C B, SILVA L A M, LEÃO V A. The effects of fluoride and aluminum ions on ferrous-iron oxidation and copper sulfide bioleaching with Sulfobacillus thermosulfidooxidans [J]. Biochemical Engineering Journal, 2012, 62: 48−55.

[11] DENG S, GU G H. An electrochemical impedance spectroscopy study of arsenopyrite oxidation in the presence of *Sulfobacillus thermosulfidooxidans* [J]. Electrochimica Acta, 2018, 287: 106−114.

[12] OJUMU T V, PETERSEN J, HANSFORD G S. The effect of dissolved cations on microbial ferrous-iron oxidation by *Leptospirillum ferriphilum* in continuous culture [J]. Hydrometallurgy, 2008, 94: 69−76.

[13] PATHAK A, MORRISON L, HEALY M G. Catalytic potential of selected metal ions for bioleaching, and potential techno-economic and environmental issues: A critical review [J]. Bioresource Technology, 2017, 229: 211−221.

[14] ZHANG L J, ZHOU W B, LI K, MAO F, WAN L L, CHEN X H, ZHOU H B, QIU G Z. Synergetic effects of *Ferroplasma thermophilum* in enhancement of copper concentrate bioleaching by *Acidithiobacillus caldus* and *Leptospirillum ferriphilum* [J]. Biochemical Engineering Journal, 2015, 93: 142−150.

[15] ZHANG Y, LI Q, LIU X L, YIN H Q, YANG Y B, XU B, JIANG T, HE Y H. The catalytic effect of copper ion in the bioleaching of arsenopyrite by Acidithiobacillus ferrooxidans in 9K culture medium [J]. Journal of Cleaner Production, 2020, 256: 120391.

[16] OJUMU T V, HANSFORD G S, PETERSEN J. The kinetics of ferrous-iron oxidation by *Leptospirillum ferriphilum* in continuous culture: The effect of temperature [J]. Biochemical Engineering Journal, 2009, 46: 161−168.

[17] PINA P S, OLIVEIRA V A, CRUZ F L S, LEÃO V A. Kinetics of ferrous iron oxidation by *Sulfobacillus thermosulfidooxidans* [J]. Biochemical Engineering Journal, 2010, 51: 194−197.

[18] NURMI P, ÖZKAYA B, KAKSONEN A H, TUOVINEN O H, PUHAKKA J A. Inhibition kinetics of iron oxidation by *Leptospirillum ferriphilum* in the presence of ferric, nickel and zinc ions [J]. Hydrometallurgy, 2009, 97: 137−145.

[19] OZKAYA B, SAHINKAYA E, NURMI P, KAKSONEN A H, PUHAKKA J A. Kinetics of iron oxidation by *Leptospirillum*

ferriphilum dominated culture at pH below one [J]. Biotechnology and Bioengineering, 2007, 97: 1121−1127.
[20] NEMATI M, HARRISON S T L, HANSFORD G S, WEBB C. Biological oxidation of ferrous sulphate by *Thiobacillus ferrooxidans*: A review on the kinetic aspects [J]. Biochemical Engineering Journal, 1998, 1: 171−190.
[21] PENEV K, KARAMANEV D. Kinetics of ferrous iron oxidation by *Leptospirillum Ferriphilum* at moderate to high total iron concentrations [J]. Advanced Materials Research, 2009, 71/72/73: 255−258.
[22] QIN W Q, LIU K, DIAO M X, WANG J, ZHANG Y S, YANG C R, JIAO F. Oxidation of arsenite (As(III)) by ferric iron in the presence of pyrite and a mixed moderately thermophilic culture [J]. Hydrometallurgy, 2013, 137: 53−59.
[23] NORRIS P R, CLARK D A, OWEN J P, WATERHOUSE S. Characteristics of *Sulfobacillus acidophilus* sp. nov. and other moderately thermophilic mineral-sulphide-oxidizing bacteria [J]. Microbiology, 1996, 142: 775−783.
[24] WATKIN E L J, KEELING S E, PERROT F A, SHIERS D W, PALMER M L, WATLING H R. Metals tolerance in moderately thermophilic isolates from a spent copper sulfide heap, closely related to Acidithiobacillus caldus, *Acidimicrobium ferrooxidans* and Sulfobacillus thermosulfidooxidans [J]. Journal of Industrial Microbiology & Biotechnology, 2009, 36: 461−465.
[25] SILVERMAN M P, LUNDGREN D G. Studies on the chemoautotrophic iron bacterium *Ferrobacillus ferrooxidans*: I. An improved medium and a harvesting procedure for securing high cell yields [J]. Journal of Bacteriology, 1959, 77: 642−647.
[26] MOLCHANOV S, GENDEL Y, IOSLVICH I, LAHAV O. Improved experimental and computational methodology for determining the kinetic equation and the extant kinetic constants of Fe(II) oxidation by *Acidithiobacillus ferrooxidans* [J]. Applied Environmental and Microbiology, 2007, 73: 1742−1752.
[27] OJUMU T V, PETERSEN J, SEARBY G E, HANSFORD G S. A review of rate equations proposed for microbial ferrous-iron oxidation with a view to application to heap bioleaching [J]. Hydrometallurgy, 2006, 83: 21−28.
[28] SUNDKVIST J E, GAHAN C S, SANDSTRÖM A. Modeling of ferrous iron oxidation by a *Leptospirillum ferrooxidans*-dominated chemostat culture [J]. Biotechnology Bioengineering, 2008, 99: 378−389.
[29] CHOWDHURY F, OJUMU T V. Investigation of ferrous-iron biooxidation kinetics by *Leptospirillum ferriphilum* in a novel packed-column bioreactor: Effects of temperature and jarosite accumulation [J]. Hydrometallurgy, 2014, 141: 36−42.
[30] PANIKOV N. Microbial growth kinetics [M]. Netherlands: Springer, 1995.
[31] HALLBERG K B, SEHLIN H M, LINDSTRÖM E B. Toxicity of arsenic during high temperature bioleaching of gold-bearing arsenical pyrite [J]. Applied Microbiology and Biotechnology, 1996, 45: 212−216.
[32] CABRERA G, GÓMEZ J M, CANTERO D. Kinetic study of ferrous sulphate oxidation of *Acidithiobacillus ferrooxidans* in the presence of heavy metal ions [J]. Enzyme and Microbial Technology, 2005, 36: 301−306.
[33] STOLZ J F, BASU P, SANTINI J M, OREMLAND R S. Arsenic and selenium in microbial metabolism [J]. Annual Review of Microbiology, 2006, 60: 107−130.
[34] LIU M S, BRANION R M R, DUNCAN D W. The effects of ferrous iron, dissolved oxygen, and inert solids concentrations on the growth of *Thiobacillus ferrooxidans* [J]. The Canadian Journal of Chemical Engineering, 1988, 66: 445−451.
[35] GOMEZ J M, CANTERO D. Modelling of ferrous sulphate oxidation by *thiobacillus ferrooxidans* in discontinuous culture: Influence of temperature, pH and agitation rate [J]. Journal of Fermentation and Bioengineering, 1998, 86(1): 79−83.
[36] BOGDANOVA T I, TSAPLINA I A, KONDRAT'EVA T F, DUDA V I, NATALYA E S, MELAMUD V S, TOUROVA T P, KARAVAIKO G I. *Sulfobacillus thermotolerans* sp. nov., a thermotolerant, chemolithotrophic bacterium [J]. International Journal of Systematic Evolutionary Microbiology, 2006, 56: 1039−1042.
[37] VITAYA V B, KOIZUMI J I, TODA K. A kinetic assessment of substantial oxidation by Sulfolobus acidocaldarius in pyrite dissolution [J]. Journal of Fermentation and Bioengineering, 1994, 77(5): 528−534.

As(III)对生物氧化 Fe^{2+}动力学的影响

魏 茜[1]，覃文庆[1]，刘学端[1]，刘 凯[2]，杨聪仁[1]

1. 中南大学 资源加工与生物工程学院，长沙 410083；2. 广西环境保护科学研究院，南宁 530022

摘 要：研究含砷金精矿溶解释放的有毒金属离子对生物氧化 Fe^{2+}的影响。考察不同初始 Fe^{2+}浓度和 As(III)浓度下中等嗜热微生物对 Fe^{2+}的氧化，并用 Monod 方程拟合不同条件下 Fe^{2+}的氧化。结果表明：Fe^{2+}氧化的速率随着初始 Fe^{2+}浓度的升高而加快，当 Fe^{2+}浓度达到 12 g/L 时，Fe^{2+}氧化速率不再升高。As(III)严重抑制 Fe^{2+}的氧化，当 As(III)浓度为 8 g/L 时，微生物完全氧化 9 g/L Fe^{2+}所需要的时间超过 200 h。生物氧化 Fe^{2+}符合 Monod 模型，在未添加 As(III)时，微生物的最大比生长速率和底物亲和常数分别为 0.142 h^{-1} 和 0.053 g/L。As(III)对 Fe^{2+}氧化的抑制属于竞争性抑制，其抑制常数为 0.0035 g/L。

关键词：中等嗜热微生物；生物氧化 Fe^{2+}；As(III)；含砷金精矿；动力学

(Edited by Xiang-qun LI)